A MODEL FOR ANALYSING THE DYNAMICS OF BELT TRANSMISSIONS WITH A 5PK BELT

KRZYSZTOF KUBAS[1]
University of Bielsko-Biała

Summary

A belt transmission model used for analysing the dynamics of such a transmission has been presented in this paper. A two-dimensional discrete model was adopted, consisting of rigid elements connected with each other by means of longitudinal and torsional spring-damping elements (SDEs). For the belt-pulley contact, a special contact model and a dry friction model were adopted. The belt-pulley contact phenomena were described with the use of a model with appropriate stiffness and damping between the contacting surfaces and a simplified Threlfall friction model was used to describe the friction phenomenon. The transmission motion caused by a force-type input or a kinematic input applied to transmission pulleys was examined. Results of determining the reaction forces developing in the belt and the normal and friction forces between the belt element and the pulley, arising from the driving and resistance torques on the pulleys, have been given as an example in the subsequent part of this article for the belt transmission adopted. Finally, an example of using the model to analyse the dynamics of an automotive belt transmission system driving the alternator and coolant pump has been presented.

Keywords: belt transmissions, dynamics analysis, dry friction, poly-V belt

1. Introduction

Nowadays, belt transmissions are becoming more and more common. The good insulation against vibrations transmitted by the driving pulley or the relatively low mass of such systems are in certain situations the factors that are decisive for the superiority of such transmissions over other systems. Undoubtedly, this growing popularity stems from their increasing reliability, which in turn is an effect of the application of better solutions, especially the belts. What is meant here is both the use of more and more reliable materials and development in the belt engineering (belt shaping, type and layout of the load-carrying layer, etc.).

The necessity of introducing steadily improved solutions is connected with a series of tests of successive prototypes, carried out on appropriate test stands. This often results

[1] University of Bielsko-Biała, Faculty of Mechanical Engineering and Computer Science, Department of Mechanics, ul. Willowa 2, 43-309 Bielsko-Biała, Poland, e-mail: kkubas@ath.bielsko.pl

in a significant growth in costs. A way to reduce the costs may be the construction of a "virtual prototype", i.e. a computer model that would enable preliminary selection of optimum belt characteristics.

The theoretical coefficient of efficiency of a belt transmission should exceed 90%. Alas, many transmissions of this kind work with an efficiency being far below this level. This may be due to a variety of factors, such as incorrect design or assembly of the transmission system (including incorrect belt tension or pulley misalignment) or improper maintenance or operation of the system. The most common faults of belt transmission operators include insufficiently frequent inspection of the transmission belt during its operation. The inspection should include not only the checking of belt tension or damage but also searching for possible contaminations. On the other hand, even such aspects might be investigated with the use of an appropriate computer model of the transmission system, e.g. for examining the impact of transmission defects on its efficiency.

Deliberations on the phenomena occurring in belt transmission systems date back to the 18th century and they were initiated by Leonard Euler [7]. The major research works carried out over the centuries, with the most important works being specified in more detail, have been presented by Fawcett in the widely quoted publication [8]. It is worth adding here that works on chain transmissions have also been discussed in that publication.

From the point of view of the assumptions made in the model presented herein, the studies where discrete belt models have been presented ([9, 13, 14]) seem to be particularly important.

Due to great complexity of the phenomena that occur in belt transmissions, the describing of friction and contact with the use of appropriate mathematical methods seems to be an extremely difficult task. In the literature, piecewise linear friction models, such as the Coulomb-like tri-linear creep-rate-dependent friction law [12, 14] or the elastic/perfectly plastic friction law (EPP) [10], are very popular. The normal forces acting on the pulley, necessary for determining the said friction forces, can be established with the use of a spring-damping model [2, 4, 14] (also referred to as a "penalty contact model"). Such a model was used in this study, too.

Moreover, a system of rigid elements connected with each other by means of spring-damping elements was adopted to represent the belt in the belt transmission model shown in this study. In transmissions of this type, the belt is subjected in most cases to significant strains caused by bending, e.g. on curved surfaces of pulleys and tensioner idlers, if any; therefore, an assumption was made that a relatively large number of elements would have to be used to discretize the belt. Obviously, this affects the computation speed and, in consequence, the time of carrying out the analyses.

In this connection, it was considered reasonable to make some preliminary assumptions at the beginning of the model development process. In particular, a planar (two-dimensional) model of the belt transmission system was adopted, with disregarding e.g. the longitudinal torsion of the belt and the impact of local phenomena (such as changes in the belt cross-section caused by wedging the belt into the pulley grove). Thus, the number

of degrees of freedom (and, in consequence, the number of generalized coordinates) of the system was reduced. Moreover, the equations of motions were thus considerably simplified, which made it possible to avoid their matrix notation. Thanks to this, the number of the computer operations that would be required e.g. due to the occurrence of the so-called "sparse arrays" could be additionally reduced. A friction model was adopted where differentiation between the phases of static and kinetic friction was not taken into account. An assumption was also made that the pulleys could be considered as perfectly circular (i.e. changes in the distance between the belt wrapping the pulley and the centre of pulley rotation could be considered as exclusively resulting from the kinematics of the belt-pulley contact phenomena). For the errors of numerical integration of the equations of motion to be minimized and for the computation process to be additionally speeded up, an assumption was made that the differential equations of motion would be solved with the use of an appropriate method with variable-step integration. With this end in view, the Runge-Kutta-Fehlberg method was used.

The assumptions as described above are often made when belt transmission models are developed. Their beneficial impact on the effectiveness of the mathematical model was analysed by e.g. Schindler in study [16].

Undoubtedly, there are many good points of the discretization of a transmission belt. They include e.g. the possibility of identifying changes in the friction forces along the circumference of a pulley or distribution of the axial forces along the entire belt length.

2. Mathematical model

The belt was assumed to consist of n_{cz} elements. Each of the elements was connected with the neighbouring ones by means of spring-damping elements (hereafter referred to as SDE) with appropriate longitudinal or torsional rigidity and damping values (Fig. 1a).

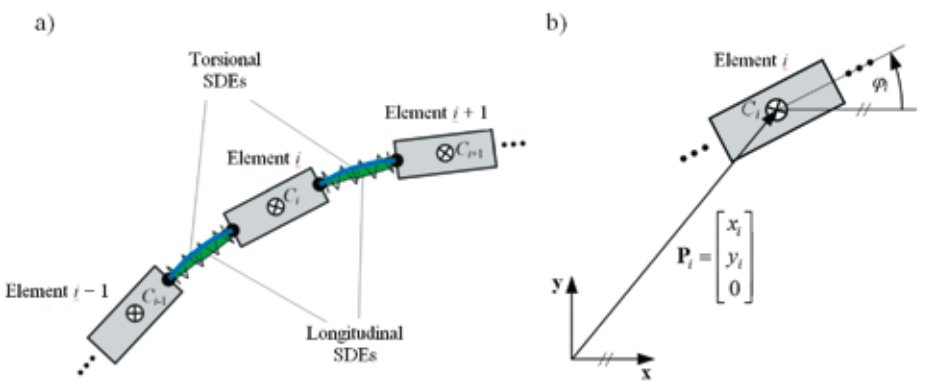

Fig. 1. The belt model assumed: a) longitudinal and torsional SDEs; b) generalized coordinates defining the location and orientation of element *i* of the belt

As mentioned above, a two-dimensional model was to represent the belt transmission system. For every element i (where i = 0...n_{cz} – 1), three generalized coordinates were adopted, i.e. displacements x_i and y_i of its centre of mass in relation to axes $\mathbf{x}$ and $\mathbf{y}$ of the global coordinate system and angle φ_i of rotation of the element in relation to its centre of mass (Fig. 1b). The value of coordinate z_i was zero. The position of the centre of mass of belt element i was defined by means of vector $\mathbf{P}_i$, as shown in Fig. 1b.

Moreover, an assumption was made that the transmission included n_k pulleys situated within plane $\mathbf{xy}$ and rotating around an axis parallel to axis $\mathbf{z}$ by angle Θ_j (where j = 0...n_k – 1). This means that the vector of the generalized coordinates could be presented in the following form:

$$\mathbf{q}^T = \left[\mathbf{q}_{cz}^T \;\vdots\; \mathbf{q}_k^T\right] = \left[x_0 \;\; y_0 \;\; \varphi_0 \;\; \ldots \;\; x_i \;\; y_i \;\; \varphi_i \;\; \ldots \;\; x_{n_{cz}-1} \;\; y_{n_{cz}-1} \;\; \varphi_{n_{cz}-1} \;\vdots\; \theta_0 \;\; \ldots \;\; \theta_j \;\; \ldots \;\; \theta_{n_k-1}\right], \tag{1}$$

where: $\mathbf{q}_{cz}$ – vector of the generalized coordinates of all the belt elements;
$\mathbf{q}_k$ – vector of the generalized coordinates of all the pulleys.

According to the assumptions made, the total number of the generalized coordinates was $3n_{cz} + n_k$.

At first, the belt was divided into n_{cz} elements. The elements of the belt modelled were assumed as homogenous segments of a mass m_i each (the thickness of the belt segments was neglected and their centres of mass were assumed as identical with their geometric centres). The mass moment of inertia of element i in relation to an axis $\mathbf{z}$ perpendicular to the plane of motion and going through the centre of mass of the said element is:

$$I_{z_i} = \frac{1}{12} m_i l_i^2, \tag{2}$$

and the total belt mass is:

$$m_p = \sum_{i=0}^{n_{cz}-1} m_i. \tag{3}$$

For a specific belt transmission case being analysed, it would be advisable to check whether the mass distribution along the entire length of the belt may be considered as uniform because if the answer to this question were affirmative then the determining of mass parameters of individual elements from equations (2) and (3) would be significantly simplified.

2.1. Model of the belt-pulley contact

For the contact between belt elements and pulleys to be taken into account in the transmission model, the vectorial notation of forces was used. A schematic diagram of the assumed system of forces acting on element i of the belt when the element is in contact with pulley j has been shown in Fig. 2.

It was assumed that the component forces, i.e. normal forces $\mathbf{N}_{ji}$ and friction forces $\mathbf{T}_{ji}$, were applied to the centre of mass of each of the belt elements being in contact with the pulley. Such an assumption is acceptable if the belt thickness is disregarded (thanks to which e.g. the nature of stresses in the belt cross-section is not analysed and the friction force may be reduced to centre C_i) and a sufficiently large number of elements is adopted to discretize the belt, which translates into sufficiently small lengths of the belt elements. It is also worth mentioning here that the assumptions made are consistent with the current trends in the designing of transmission belts, according to which the belt height is minimized to reduce the transverse deformations and thus to increase the transverse stiffness of the belt [6].

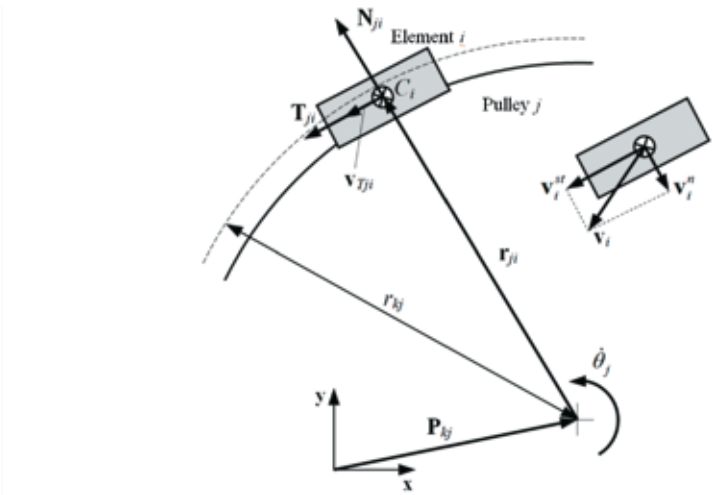

Fig. 2. The assumed system of belt element *i* velocity components and forces applied to this belt element by pulley *j*

As it can be seen in Fig. 2, vector $\mathbf{r}_{ji}$ was drawn from the centre of pulley j to the centre of mass of belt element i. At the instant when the belt element comes into contact with the pulley but the value of normal force $\mathbf{N}_{ji}$ is still zero, the length of this vector is equal to an arbitrarily selected value r_{kj}. Hence, for a non-zero normal force, the following inequality holds: $r_{ji} < r_{kj}$. The position of the pulley centre in the global coordinate system was defined by vector $\mathbf{P}_{kj}$.

Vector $\mathbf{r}_{ji}$ may be determined from the equation:

$$\mathbf{r}_{ji} = \mathbf{P}_i - \mathbf{P}_{kj}. \tag{4}$$

The versor consistent with the direction and sense of vector $\mathbf{r}_{ji}$ is equal to:

$$\hat{\mathbf{r}}_{ji} = \frac{\mathbf{r}_{ji}}{\left|\mathbf{r}_{ji}\right|}. \tag{5}$$

The depth of penetration between belt element i and pulley j may be determined from the formula:

$$p_{ji} = r_{kj} - \left|\mathbf{r}_{ji}\right|. \tag{6}$$

At an assumption that the linear velocity of the pulley centre is equal to zero, the value of penetration velocity $\dot{p}_{ji}$ may be considered as equal to the value of the radial velocity component $\mathbf{v}_i^n$ (Fig. 2). This value was determined from the following scalar product:

$$\dot{p}_{ji} = \left|\mathbf{v}_i^n\right| = -\mathbf{v}_i \cdot \hat{\mathbf{r}}_{ji}^T, \tag{7}$$

where: $\mathbf{v}_i$ – velocity of the centre of mass of belt element i.

The direction of normal force $\mathbf{N}_{ji}$ resulting from the contact between belt element i and pulley j is consistent with that of radial versor $\hat{\mathbf{r}}_{ji}$; therefore, we have the following:

$$\mathbf{N}_{ji} = N_{ji}\hat{\mathbf{r}}_{ji}. \tag{8}$$

The value of this force was determined in a form similar to that presented in study [3], where the non-linear relationship between deformation and force was proven:

$$N_{ji}\left(p_{ji}, \dot{p}_{ji}\right) = c_1 \cdot p_{ji}^2 + c_2 \cdot p_{ji} + \delta\left(p_{ji}\right) \cdot b \cdot \dot{p}_{ji}, \tag{9}$$

where: c_1, c_2 – stiffness coefficients of the belt-pulley contact;
b – damping coefficient of the belt-pulley contact.

A graphical representation of the function $\delta(p_{ji})$ used in equation (9) has been presented in Fig. 3.

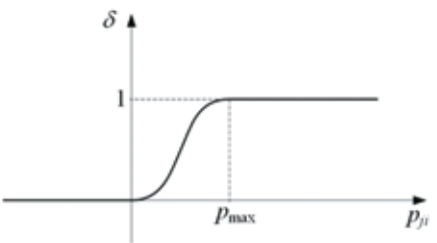

Fig. 3. Graphical representation of the function $\delta(p_{ji})$

In this model, an assumption has been made that for $p_{ji} \leq 0$, the force $\mathbf{N}_{ji}$ will be equal to zero. At the instant when the contact just begins, i.e. when p_{ji} is still very close to zero, only the elasticity has an effect. Thanks to the function $\delta(p_{ji})$ being applied, the damping effect rises (from 0 to b) within the interval $0 < p_{ji} < p_{max}$ to reach the "full damping" level (i.e. the level at which the full value of the b coefficient is taken to the calculation formula) when an arbitrarily chosen value p_{max} is exceeded. Such an approach made it possible, *inter alia,*

to avoid the effect of the belt and pulley being "stuck" together at the beginning of contact between them (especially when the velocity $\dot{p}_{ji}$ is relatively high).

For the damping to change smoothly from zero to its full value (as shown in Fig. 3), the function $\delta(p_{ji})$ representing this transition was described as a function of state having the form of constant values and a third degree polynomial in three predefined intervals:

$$\delta\left(p_{ji}\right)=\begin{cases}0 & for\ p_{ji}\le 0,\\ \left(\dfrac{p_{ji}}{p_{max}}\right)^2\left(3-2\dfrac{p_{ji}}{p_{max}}\right) & for\ 0<p_{ji}<p_{max},\\ 1 & for\ p_{ji}\ge p_{max}.\end{cases} \tag{10}$$

Thanks to the application of formulas (9) and (10), the force component resulting from damping at the belt and pulley interface depends not only on the penetration velocity $\dot{p}_{ji}$ but also on the penetration depth p_{ji}. It should be simultaneously stressed that these relationships are universally used in models of contact. A similar model has been used e.g. in the MSC.ADAMS software [19].

2.2. Model of friction

The friction force was determined with the use of a model based on a simplified characteristic of the coefficient of friction. The static friction phase, which is normally taken into account in the classical approach but the modelling of which is particularly difficult because of a change in the form and number of the equations to be solved, has been skipped in this model. In the case of contact between two mating surfaces, the equations of statics must be formulated and the friction force is determined from such equations; if the surfaces move in relation to each other, however, then the friction force is known and differential equations of motion have to be formulated. It should be stressed here that when the differential equations of motion are integrated then the instants of change in the friction state are difficult for identification. The skipping of the static friction phase is possible thanks to the fact that the coefficient of friction depends on the value of the relative velocity v of mating elements at the belt-pulley interface. The Coulomb formula, used for determining the value of friction force $\mathbf{T}$, takes the following form in this case:

$$T=\mu(v)\cdot N. \tag{11}$$

Fig. 4 shows the simplified form of the coefficient of friction as adopted by Threlfall [17]. As it can be seen in the graph, the value Δv is an arbitrarily chosen level of the velocity v, from which the coefficient of friction is assumed to take the value of μk appropriate for kinetic friction.

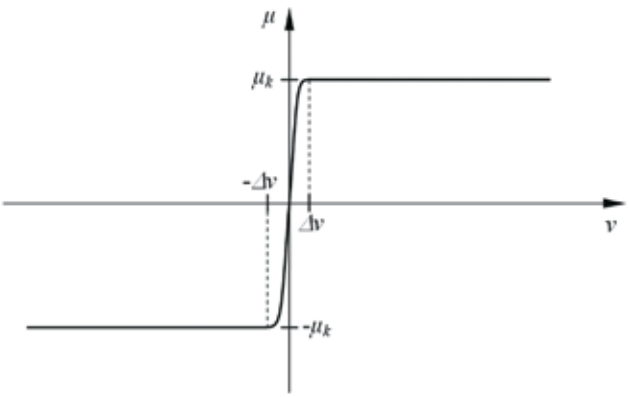

Fig. 4. Simplified form of the characteristic curve of the coefficient of friction [17]

The above characteristic curve is usually adopted with assuming identical values for the static and kinematic friction ($\mu_s = \mu_k$). As it has been shown in publication [3], the values of these coefficients may actually be close to each other; therefore, a decision was made to use a simplified model presented in Fig. 4 in this work as well. The smooth transition between values $-\mu_k$ and μ_k was obtained by applying a third order curve in a form similar to that represented by equation (10).

The assumptions made are, in a way, inconsistent with the traditional approach to the friction issues, because in most cases the static friction is taken as exclusively occurring when the velocity is equal to zero. In reality, however, micro-displacement, also referred to as "micro-slip" or "preliminary displacement", occurs in the state when two mating surfaces are stuck together. For the first time, this phenomenon was more comprehensively investigated by Wierchowski and Rankin, separate from each other, in 1926 [11] and it was the subject matter of many research works, which resulted in e.g. the publication by Bowden and Tabor [1], already considered a classic, or the widely quoted report by Dahl [5]. The oldest publication of those known to the author and pertinent to these issues, where results of research works confirming the existence of the phenomenon of micro-displacements in belt transmissions were presented, is the study by Reynolds [15] dated 1847.

In the case under consideration, for this very flexible contact between the surfaces of a rubber transmission belt and a steel pulley, an assumption should be made that within the velocity range of up to certain Δv values, the micro-displacement phenomenon will take place, because in most cases (except the case of a toothed belt) the slipping (including micro-displacement) takes place between the belt and the pulley, although it is different for different belt types. Obviously, the intensity of occurrence of this phenomenon for a specific belt transmission type may only be evaluated after appropriate experimental tests are carried out (this will probably be the subject matter of further author's investigations into the issues under consideration. The question how much the friction characteristics may differ from each other for various belt types may be well illustrated

e.g. by examples of different assumptions made for different friction models adopted (where the characteristics are taken as functions of different variables, of different degree of non-linearity), as presented in publications [3, 9, 14]. Some of them are relationships defined experimentally.

For the values of the coefficient of friction to be determined, the vector of linear velocity of the segment of pulley j at the point of contact with element i of the belt had to be defined:

$$\mathbf{v}_{kj} = \dot{\boldsymbol{\theta}}_j \times \hat{\mathbf{r}}_{ji}, \tag{12}$$

where:

$\dot{\boldsymbol{\theta}}_j = \begin{bmatrix} 0 \\ 0 \\ \dot{\theta}_j \end{bmatrix}$ – vector of the angular velocity of pulley j.

When the case of friction between belt element i and a pulley is analysed, the tangential component of the vector representing the velocity of the centre of belt element mass should be determined as well:

$$\mathbf{v}_i^{st} = \left(\mathbf{v}_i \cdot \hat{\boldsymbol{\tau}}_{ji}^T\right)\hat{\boldsymbol{\tau}}_{ji}. \tag{13}$$

In the above equation, versor $\hat{\boldsymbol{\tau}}_{ji}$ parallel to the tangent going through the centre of mass of belt element i must be known; this versor may be determined from the following formula:

$$\hat{\boldsymbol{\tau}}_{ji} = \frac{\boldsymbol{\tau}_{ji}}{\left|\boldsymbol{\tau}_{ji}\right|} = \frac{\hat{\mathbf{Z}} \times \hat{\mathbf{r}}_{ji}}{\left|\boldsymbol{\tau}_{ji}\right|}. \tag{14}$$

The angle between versors $\hat{\mathbf{Z}}$ and $\hat{\mathbf{r}}_{ji}$ is invariably equal to 90° (because, as previously mentioned, the pulley is situated within plane $\mathbf{xy}$ and its axis of rotation is parallel to axis $\mathbf{z}$); therefore, $\left|\hat{\mathbf{Z}} \times \hat{\mathbf{r}}_{ji}\right| = 1$ and formula (14) may be reduced to the form as follows:

$$\hat{\boldsymbol{\tau}}_{ji} = \hat{\mathbf{Z}} \times \hat{\mathbf{r}}_{ji}. \tag{15}$$

In practice, when the pulley is moving, the direction and sense of versor $\hat{\boldsymbol{\tau}}_{ji}$ are consistent with the direction and positive sense, respectively, of velocity vector $\mathbf{v}_{kj}$. However, when pulley j is at a standstill (i.e. when $\mathbf{v}_{kj}$ = 0), then the direction tangential to the pulley circumference can be identified by means of $\hat{\boldsymbol{\tau}}_{ji}$ (in such a case, the versor cannot be determined from the zero vector $\mathbf{v}_{kj}$).

Hence, the relative velocity between the rubbing elements (shown in Fig. 2) is:

$$\mathbf{v}_{Tji} = \mathbf{v}_{kj} - \mathbf{v}_i^{st}. \tag{16}$$

The friction force was defined by the equation:

$$\mathbf{T}_{ji} = \boldsymbol{\mu}\left(\mathbf{v}_{Tji}\right) \cdot N_{ji}, \tag{17}$$

where: $\boldsymbol{\mu}(\mathbf{v}_{Tji}) = \mu(v_{Tji})\hat{\mathbf{v}}_{Tji}$ – coefficient of friction in vectorial notation;
$\hat{\mathbf{v}}_{Tji}$ – versor whose direction and sense are consistent with those of vector $\mathbf{v}_{Tji}$.

It can be noticed that the above equation is a modified form of equation (11).

In the friction model adopted, the presence of separate static contact and slip zones on the pulley circumference was ignored. The author is aware of the fact that the taking of such zones into account would improve the accuracy of representation of the phenomena occurring at the belt-pulley interface; therefore, this issue is to be considered at his subsequent works.

2.3. Equations of motion

Fig. 5 shows a schematic diagram of the adopted system of forces and moments applied to belt element i by the neighbouring belt elements.

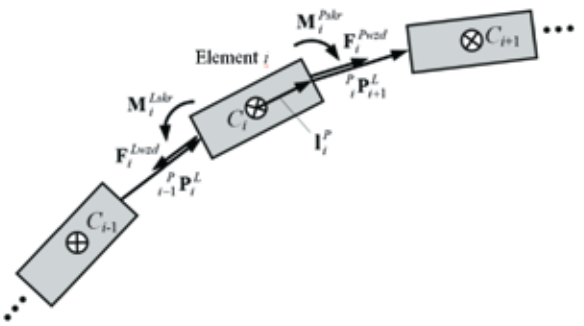

Fig. 5. System of forces and moments applied to belt element *i* by the neighbouring elements

The values of the reaction forces and moments in the longitudinal and torsional SDEs that connect element i – 1 with element i were described by equations known in the literature as the Kelvin-Voigt equations [18]:

$$F_i^{Lwzd} = F_{i-1}^{Pwzd} = c_{wzd}\left(\Delta l_i^L\right)^{e_{wzd}} + b_{wzd}\Delta \dot{l}_i^L, \tag{18}$$

$$M_i^{Lskr} = M_{i-1}^{Pskr} = c_{skr}\left(\varphi_i - \varphi_{i-1}\right)^{e_{skr}} + b_{skr}\left(\dot{\varphi}_i - \dot{\varphi}_{i-1}\right), \tag{19}$$

where: F_i^{Lwzd}, F_i^{Pwzd} – values of the reaction forces in the left and right longitudinal SDE (that connect belt element i with element i – 1 and belt element i with element i + 1, respectively);

M_i^{Lskr}, M_i^{Pskr} – values of the torsional moments in the left and right torsional SDE, respectively;

c_{wzd}, b_{wzd} – stiffness and damping coefficient, respectively, of the longitudinal SDE of the belt;

c_{skr}, b_{skr} – stiffness and damping coefficient, respectively, of the torsional SDE of the belt;

e_{wzd}, e_{skr} – exponential coefficients being measures of the longitudinal and torsional stiffness, respectively, of the SDE of the belt;

$\Delta l_i^L = \Delta l_{i-1}^P = \left| {}_{i-1}^{P}\mathbf{P}_i^L \right|$ – deformation of the longitudinal SDE of the belt;

$\Delta \dot{l}_i^L = \Delta \dot{l}_{i-1}^P = v_i^{L'} - v_{i-1}^{P'}$ – rate of deformation of the longitudinal SDE of the belt;

$v_i^{L'} = \mathbf{v}_i^L \cdot \left({}_{i-1}^{P}\hat{\mathbf{P}}_i^L \right)^T$, $v_{i-1}^{P'} = \mathbf{v}_{i-1}^P \cdot \left({}_{i-1}^{P}\hat{\mathbf{P}}_i^L \right)^T$ – projections of velocity vectors $\mathbf{v}_i^L$ and $\mathbf{v}_{i-1}^P$ on vector ${}_{i-1}^{P}\mathbf{P}_i^L$;

${}_{i-1}^{P}\hat{\mathbf{P}}_i^L$ – versor whose direction and sense are consistent with those of vector ${}_{i-1}^{P}\mathbf{P}_i^L$.

Vector ${}_{i-1}^{R}\mathbf{P}_i^L$ may be determined with the use of the following equation:

$$ {}_{i-1}^{R}\mathbf{P}_i^L = \mathbf{P}_i - \mathbf{l}'_i - \mathbf{P}_{i-1} + \mathbf{l}'_{i-1}. \tag{20} $$

where:

$$ \mathbf{l}'_i = \begin{bmatrix} \frac{l_i}{2}\cos\varphi_i \\ \frac{l_i}{2}\sin\varphi_i \\ 0 \end{bmatrix} $$

– vector defining the direction and half-length of belt element i (vector $\mathbf{l}'_{i-1}$ is determined likewise).

Force $\mathbf{F}_i^{Lwzd}$ has identical direction but opposite sense to those of vector ${}_{i-1}^{P}\mathbf{P}_i^L$, while both the direction and sense of force $\mathbf{F}_i^{Pwzd}$ are consistent with those of vector ${}_{i}^{P}\mathbf{P}_{i+1}^L$. As it can be seen in Fig. 5, these vectors define the directions, senses, and magnitudes of elongation of the SDEs that connect belt element $i-1$ with element i and element i with element $i+1$.

The equations of motion were derived with the use of the Newton-Euler formalism. The equations of motion of belt element i take the form:

$$ \begin{cases} m_i \ddot{x}_i = (\mathbf{F}_i^{Lwzd} + \mathbf{F}_i^{Pwzd} + \sum_{j=0}^{n_i-1}(\mathbf{N}_{ji} + \mathbf{T}_{ji}) + m_i\mathbf{g}) \cdot \hat{\mathbf{X}}^T, \\ m_i \ddot{y}_i = (\mathbf{F}_i^{Lwzd} + \mathbf{F}_i^{Pwzd} + \sum_{j=0}^{n_i-1}(\mathbf{N}_{ji} + \mathbf{T}_{ji}) + m_i\mathbf{g}) \cdot \hat{\mathbf{Y}}^T, \\ I_{z_i} \ddot{\varphi}_i = (\mathbf{M}_i^{Lwzd} + \mathbf{M}_i^{Pwzd} + \mathbf{M}_i^{Lskr} + \mathbf{M}_i^{Pskr}) \cdot \hat{\mathbf{Z}}^T, \end{cases} \tag{21} $$

where: $\hat{\mathbf{X}}^T = [1\,0\,0]$, $\hat{\mathbf{Y}}^T = [0\,1\,0]$, $\hat{\mathbf{Z}}^T = [0\,0\,1]$ – versors whose directions and senses are consistent with those of axes $\mathbf{x}$, $\mathbf{y}$, and $\mathbf{z}$ of the global coordinate system;

$\mathbf{M}_i^{Lwzd} = -\mathbf{l}_i' \times \mathbf{F}_i^{Lwzd}$;

$\mathbf{M}_i^{Pwzd} = \mathbf{l}_i' \times \mathbf{F}_i^{Pwzd}$;

$\mathbf{g}$ – acceleration of gravity.

As it can be easily noticed, equations (21) can be simplified. So, appropriate components of the vectors specified in brackets should be substituted on the right side of the equality signs.

It was assumed that the pulleys would move under the impact of driving torques applied. The equation of motion of pulley j will have the form:

$$I_{z_j}\ddot{\theta}_j = M_{nj} - \sum_{i=0}^{n_{zz}-1} \mathbf{M}_{Tji} \cdot \hat{\mathbf{Z}}^T, \tag{22}$$

where: I_{z_j} – mass moment of inertia of pulley j;
M_{nj} – driving torque value;
$\mathbf{M}_{Tji} = \hat{\mathbf{r}}_{ji} \times \mathbf{T}_{ji}$ – moment of the friction force resulting from the impact of belt element i on the pulley

As mentioned previously, the differential equations of motion were solved with the use of the Runge-Kutta-Fehlberg method with variable-step integration. The calculation results were generated in the form of appropriate time histories with the use of the MATLAB environment.

3. Verification of the model

When the model was prepared as described above, then the parameters of the transmission system described in publication [2] were applied to it as an input, with taking into account both the geometrical parameters of the transmission that was there analysed and its physical data given below, including the stiffness and damping characteristics of the belt and the parameters of friction and contact at the belt-pulley interface:

$c_{wzd} = 10^4$ N/m, $b_{wzd} = 0.5$ Ns/m, $c_{skr} = 0.0208$ Nm/rad,
$b_{skr} = 0$, $c_1 = 0$, $c_2 = 5 \cdot 10^6$ N/m,
$b = 300$ Ns/m, $p_{max} = 0.001$ m, $\Delta v = 10^{-5}$ m/s,
$\Delta_{max} = 10^{-4}$ m, $m_i = 1.036 \cdot l_i$ kg, $I_{z_1} = I_{z_2} = 0.02$ kgm^2.

Moreover, the time histories of the kinematic input on the driving pulley and of the resistance torque on the driven pulley were adopted as identical to those reported in publication [2]. These time histories have been presented in Figs. 6a and 6b, respectively.

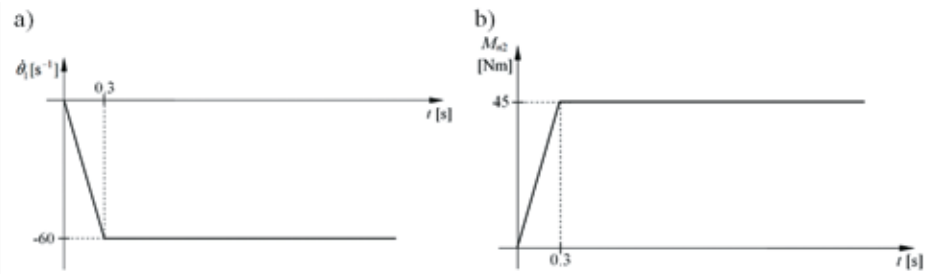

Fig. 6. Time histories of the inputs applied as adopted in this work: a) angular speed of the driving pulley; b) resistance torque on the driven pulley

In order to verify the model discussed herein, the said kinematic input had to be introduced in place of the differential equation of motion of the driving pulley. In consequence, the number of the equations of motion was reduced by one.

A graphical comparison between time histories of the angular speed of the driven pulley, recorded on an appropriate test stand by the Authors of publication [2] and obtained from the model discussed herein, has been shown in Fig. 7. The presented fragment of the angular speed vs. time curves visualizes the torsional vibrations of the driven pulley that were induced by changes in the shape of the input speed and resistance torque curves at the instant of 0.3 s.

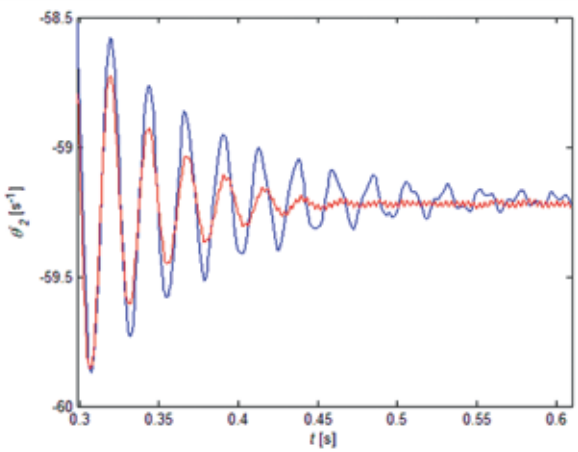

Fig. 7. Comparison between time histories of the angular speed of the driven pulley: —— reference curve [2]; —— curve obtained from the model

The curves presented show quite good conformity of the results obtained with the slip value read out from a graph and with the vibration frequency. At the same time, the belt model presented herein was found to produce a stronger vibration attenuation effect, which was reflected in the graph above in lower vibration amplitudes and a shorter vibration damping

time. Investigation into the reasons for these differences will be a subject matter of further author's research work.

4. Results of the analyses

As the next step, a belt transmission system and belt parameters based on publications [2, 3, 4] were adopted. In the works described there, the Authors took on the task to determine the parameters of longitudinal and torsional stiffness of the belt and the parameters that were necessary for taking into account the phenomena related to the belt-pulley contact, i.e. the stiffness and damping in the model of this contact and the coefficients of friction. Following the information provided in publications [3, 4], the analysis was carried out for a multi-rib belt (also referred to as serpentine belt, multi-grooved belt, poly-V belt, etc.) model 5pk, of 1.2 m total length. Belts of this type are used in transmission systems that are heavily loaded and/or operate in the conditions of high rotational speeds. The transmission system specifications were adopted in accordance with the data provided in publication [4]. There were no tensioners in the transmission system under analysis and the driving and driven pulleys had identical radii equal to $r_{k1} = r_{k2} = r_k = 0.027$ m. The distance between pulley centres was $l_p = 0.515$ m. Since the pulley radii were relatively small, the belt had to be discretized with the use of an adequately large number of elements, which was chiefly determined by the requirement of appropriate (satisfactory) representation of belt curvatures on pulley circumferences. As it was found during the experiments carried out, this had a significant impact on the accuracy of representation of the phenomena that took place in the belt-pulley contact zone, e.g. belt slip. Finally, the belt model adopted for analyses consisted of 150 elements of identical length.

It should also be mentioned that changes in the Δv value (providing that they were sufficiently small) did not significantly affect the results of the analyses carried out.

The belt was pre-tensioned to a belt force exceeding 550 N. The parameters of the transmission system subjected to the analysis were adopted in accordance with the information found in publication [3]:

$c_{wzd} = 1.52 \cdot 10^5$ N/m, $b_{wzd} = 20.5$ Ns/m, $c_{skr} = 0.026$ Nm/rad,
$b_{skr} = 0$, $c_1 = 3.0256 \cdot 10^9$ N/m^2, $c_2 = 6.5 \cdot 10^5$ N/m,
$b = 300$ Ns/m, $p_{max} = 0.001$ m, $\Delta v = 10^{-5}$ m/s,
$\Delta_{max} = 10^{-4}$ m, $m_i = 0.096 \cdot l_i$ kg.

The values of the coefficients of friction were assumed to be identical for both pulleys and they were adopted as $\mu_s = \mu_k = 1$.

The global coordinate system was so established that its origin coincided with the centre of the driving pulley, axis **y** was directed oppositely to the gravitation force vector (i.e. upwards), and axis **x** was directed towards the centre of the driven pulley. The adopted parameters of the belt transmission under analysis together with the global coordinate system have been schematically presented in Fig. 8.

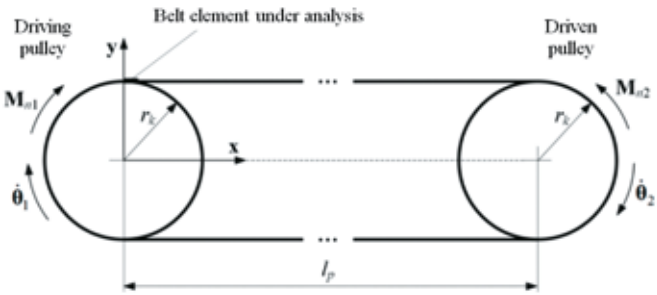

Fig. 8. The adopted parameters of the belt transmission system under analysis

As already mentioned at the discussion of the equations of motion, a force-type input in the form of a driving torque was adopted for the analysis. The driving torque $\mathbf{M}_{n1}$ on the driving pulley was represented by the torque vs. time curve shown in Fig. 9a (the direction and sense of this torque have been shown in Fig. 8). According to these assumptions, the driving torque was to grow within a time of 0.3 s to a level of 15 Nm and after this time, this torque value was to remain constant.

Moreover, the value of the resistance torque $\mathbf{M}_{n2}$ on the driven pulley was assumed to depend on the angular speed of that pulley and the torque value of 15 Nm (i.e. equal to that of the driving torque on the driving pulley) was to be reached at a pulley speed of 4 revs/s. A curve representing this torque has been shown in Fig. 9b (the direction and sense of this torque have been shown in Fig. 8). As it can be seen in the graphs, the driving and resistance torques were realized in the form of a piecewise linear function and a linear function, respectively.

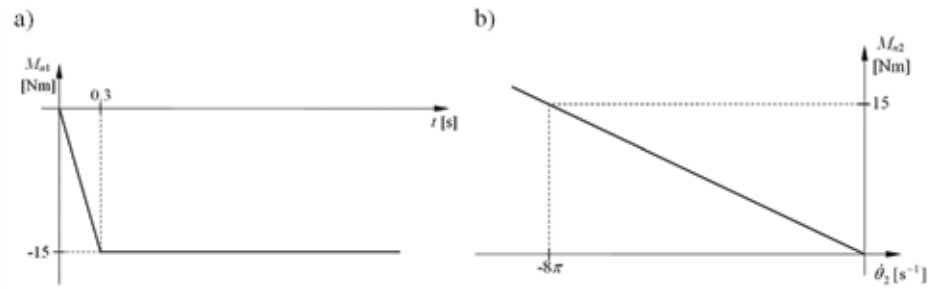

Fig. 9. Curves adopted to represent the input torques: a) driving torque on the driving pulley vs. time; b) resistance torque on the driven pulley vs. angular speed

In the case of an ideal belt transmission system without micro-displacement or slip of the belt, the values of the initial belt tension and of the driving and resistance torques adopted as described above should cause the reaction forces in the driving side of the belt to be approximately doubled in relation to the initial belt tension and the forces in the slack side to be reduced almost to zero. Due to the micro-displacements, slips, and vibrations that occur at the belt-pulley interface, this disproportion is reduced.

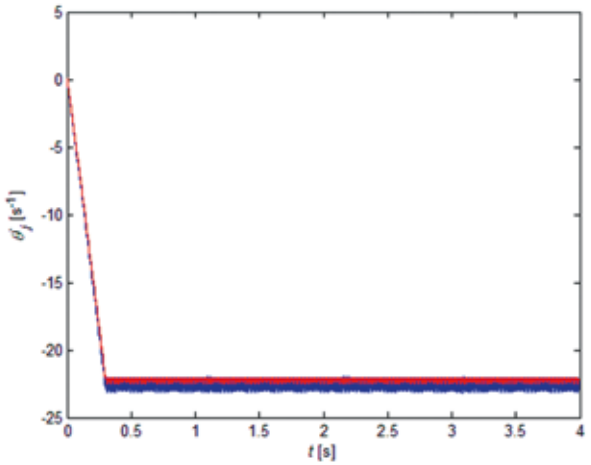

Fig. 10. Time histories of the angular velocities of the transmission pulleys, as obtained from the model: a) —— driving pulley; b) —— driven pulley

In result of the application of preset driving and resistance torques as an input, specific motion of the belt transmission system was obtained. The resulting angular speeds of the driving and driven pulleys have been graphically presented in Fig. 10. It can be seen that when the test time exceeded 0.3 s (which corresponded to a growth in the torque value to about 15 Nm), the growth in the transmission speed stopped at a level of about –22 rad/s. This value was lower than could be expected, based on the curves representing the inputs applied. The maximum speed was below the anticipated level because of energy dissipation in the SDEs in result of friction and damping in the belt-pulley contact model.

It should be pointed out here that when the transmission speed reached the appropriate (assumed) level, the slip ratio was lower than 1.5 %. This slip ratio value may depend on the assumed resistance torque and initial belt tension; nevertheless, it may also depend on the assumptions made at the model construction, including e.g. the friction and contact parameters. As mentioned previously, these issues will be the subject matter of subsequent author's studies.

It was found reasonable to pay special attention to a specific belt element (marked in Fig. 8) taken together with the SDE being next to it to obtain the time histories of the forces applied to these parts by the pulleys and neighbouring belt elements.

Fig. 11 shows the time history of the value of the reaction force in the selected longitudinal SDE (the position of this element at the initial instant has been illustrated in Fig. 8).

As it can be seen in the graph, the force value changed stepwise. At the initial instant, when the transmission began its operation, a short period of system stabilization took place. Within the time range of up to 0.75 s, the SDE under analysis remained on the slack (upper) side of the belt. At this stage, when the full working speed was achieved, the force in the belt was equal to about 250 N. After this period, the force value rapidly rose to a level

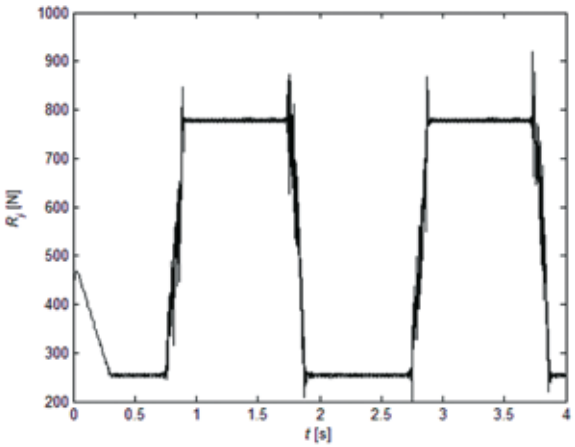

Fig. 11. Time history of the value of the reaction force in the selected longitudinal SDE, as obtained from the model

of about 780 N and remained on this level in the time interval from about 0.9 s to about 1.74 s. This was the time when the SDE was on the driving (lower) side of the belt. The next parts of the curve indicate that the SDE alternately went from the driving side to the slack side and vice versa. The time intervals during which the force in the belt rapidly changed corresponded to the relatively short periods when the belt element under analysis was in contact with the transmission pulleys.

The next curves represent the values of the normal forces applied by the pulleys to the selected belt element (Fig. 12) and the values of the friction forces (Fig. 13) generated in result of the action of the normal forces.

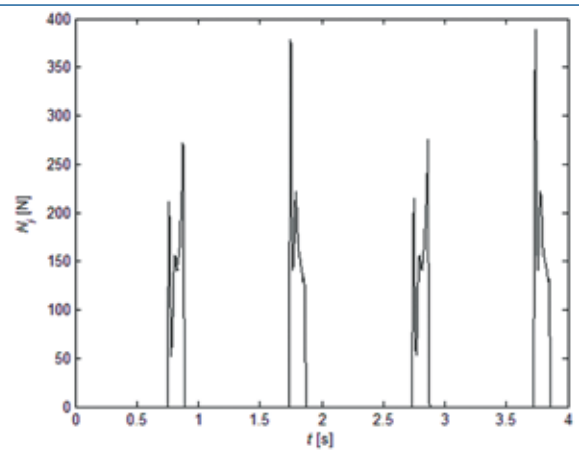

Fig. 12. Time history of the value of the normal forces applied by the pulleys to the selected belt element, as obtained from the model

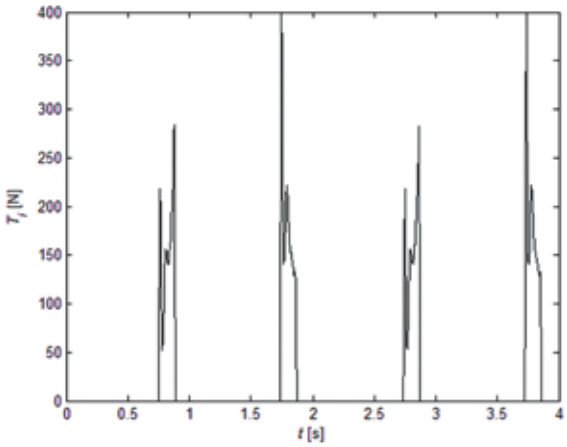

Fig. 13. Time history of the value of the friction forces at the contact between the pulleys and the selected belt element, as obtained from the model

According to the general knowledge of belt transmissions, available e.g. from publication [6], the normal force gradually decreases along the circumference of the driving pulley (observed in the direction from the driving side to the slack side of the belt) and gradually increases along the circumference of the driven pulley (observed in the direction from the slack side to the driving side of the belt). Such a relationship can be noticed in Fig. 12. In the graph, the belt element under consideration first goes through the contact with the driven pulley (see the first fragment representing the non-zero increasing values of the normal forces) and then it goes through the contact with the driving pulley (see the second fragment representing the non-zero decreasing values of the normal forces). Since the coefficients of static and kinetic friction, taken from publication [3], were close to unity, the significant similarity between the two time histories presented above may only have arisen from the fact that full static friction or kinetic friction predominated in the phenomena under analysis.

5. Example belt transmission with a 5pk belt

An example of using the mathematical methods presented to analyse the dynamics of an automotive belt transmission system driving the alternator and coolant pump has been described below. The layout of the transmission system components taken into consideration has been illustrated in Fig. 14. As it can be seen, the transmission system included engine crankshaft, alternator, and coolant pump pulleys rotating clockwise and a tensioner idler rotating anticlockwise. The origin of the global coordinate system was adopted as coinciding with the centre of the alternator pulley.

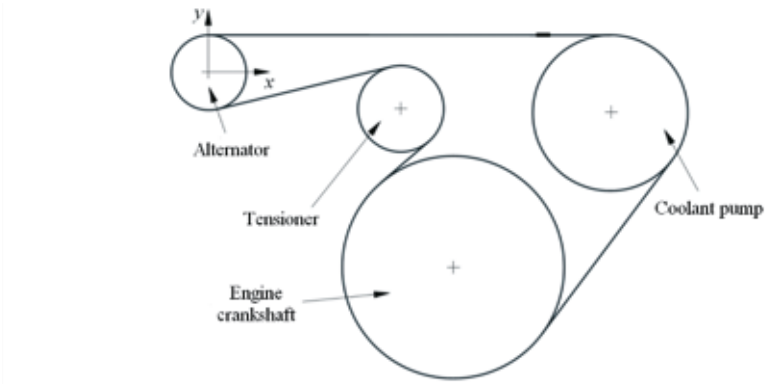

Fig. 14. Schematic diagram of an automotive belt transmission system with a 5pk belt, taken as an example

The pulley radii were adopted as follows:
- engine crankshaft r_1 = 0.08 m;
- alternator r_2 = 0.027 m;
- coolant pump r_3 = 0.056 m;
- tensioner r_4 = 0.031 m.

The belt pretensioning force was adopted as 550 N. The values of the parameters of stiffness and longitudinal and torsional damping of the SDEs and of the friction and contact between the belt and the pulleys were adopted as identical to those adopted in the preceding example. Due to the unavailability of data on the friction and contact between the belt and the tensioner idler, these data were assumed as having the same values as those of flat-belt pulleys. One should be aware, however, that the model would be more reliable if the data adopted were supplemented e.g. in accordance with information obtained from rig tests.

Moreover, the time history of of the driving torque applied to the engine crankshaft pulley was adopted as having the same form as that presented in Fig. 9a. For the needs of the analyses described herein, an assumption was made that the other pulleys and the tensioner idler would remain idle.

The time histories of the angular speeds of the pulleys and the tensioner idler have been presented in Fig. 15. It can be seen in the graph that the values of angular speed of the engine crankshaft, alternator, and coolant pump pulleys have been shown as negative while the tensioner idler has been shown to rotate with positive angular speed values. This is because the positive sign was given to the anticlockwise direction of rotation and the clockwise direction of rotation was considered negative. After a period of 0.5 s, the angular speed of the engine crankshaft pulley was stabilized on a level of about 20 rad/s, at which an equilibrium was reached between the constant driving torque and the transmission resistance to motion.

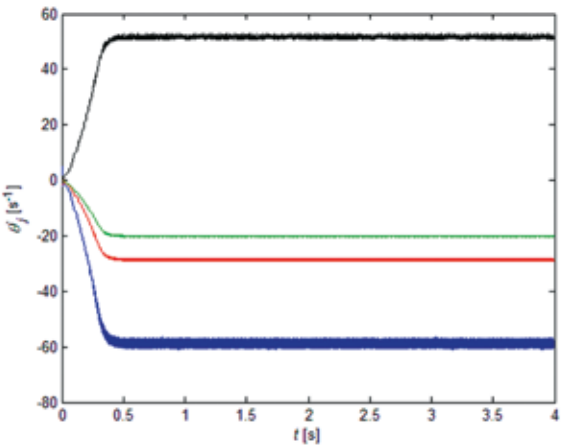

Fig. 15. Time histories of the angular speeds of the following transmission components, as obtained from the model: a) —— engine crankshaft pulley; b) —— alternator pulley; c) —— coolant pump pulley; d) —— tensioner idler

Fig. 16 shows the time history of the values of the normal forces applied by the pulleys to the selected belt element, as obtained from the model (the position of this element at the initial instant has been illustrated in Fig. 14).

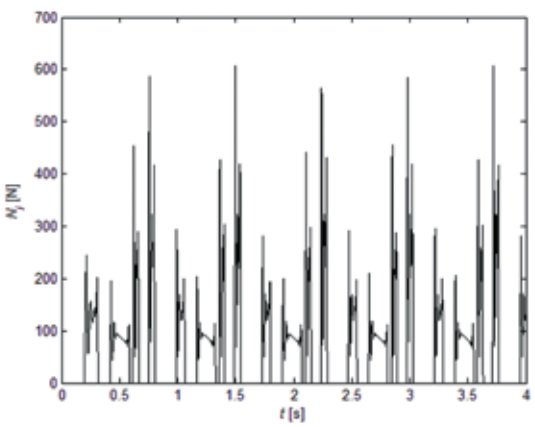

Fig. 16. Time history of the value of the normal forces applied by the pulleys to the selected belt element, as obtained from the model

The strongest normal forces occurred at the alternator pulley and, ranked second, at the tensioner idler, where their values reached levels of up to about 600 N and up to about 450 N, respectively. In this analysis, the factor that was decisive for the normal force value was the pulley radius. Actually, the alternator pulley and tensioner idler radii were the smallest.

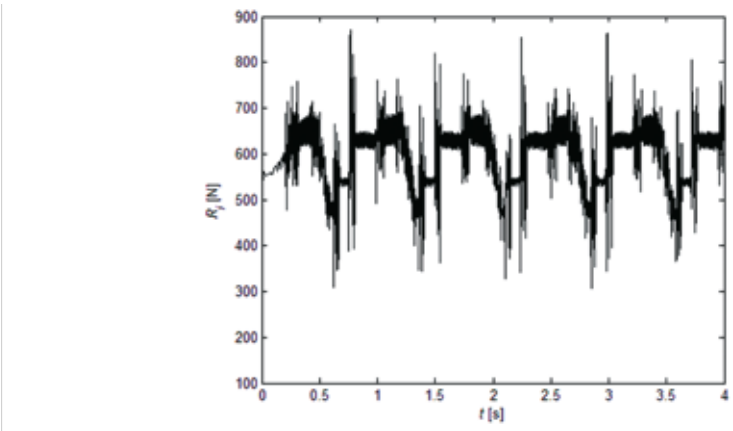

Fig. 17. Time history of the value of the reaction force in the selected longitudinal SDE, as obtained from the model

Fig. 17 shows the time history of the values of the reaction force in the selected longitudinal SDE. Short periods of the DSE under analysis moving between the transmission pulleys (although not so clearly visible as those in Fig. 11) can be noticed again as fragments of the curve representing constant values of the reaction force.

6. Recapitulation

The belt transmission model proposed and the analysis results presented as an example cannot be considered as exhausting the subject matter discussed; they should only be considered as the initiation of author's investigations into these issues. Undoubtedly, the application of a friction model with the micro-displacement phenomena being taken into account offers many possibilities but it should be stressed that they should be supported by results of scientific experiments. A matter of special importance would be the acquisition of knowledge of the parameters that describe the physical properties of a belt, including its stiffness and damping characteristics, as well as knowledge of the phenomena of friction and contact between the belt and pulleys or tensioner idlers. Investigations of this kind were already carried out, e.g. by the authors of the publications referred to herein [3, 4].

It is essential that the model should be so designed that, apart from being sufficiently sophisticated (with a discrete model having been adopted and with the friction with micro-displacement and contact phenomena having been taken into account), it should ensure relatively high numerical efficiency. Within the subsequent part of the work having been undertaken, the author is going to focus on the application of multi-thread approach to the determining of the forces of contact of individual belt elements with the pulley, while this, according to the Author of publication [16], considerably affects the computation speed. This is because the computer application thus designed would be better adapted

to multicore processors, which are now most often used in computers (the calculation of contact forces may be divided among several cores operating in parallel).

Undoubtedly, the model proposed can be further developed. In author's opinion, particularly interesting would be an analysis of the case where a part of the belt would be contaminated e.g. by an oil film. Such a situation can be very dangerous because it may cause not only a growth in the belt slip but also increased wear of the uncontaminated belt parts, which means uneven belt wear. For such a problem to be tackled, a small modification of the model would be needed, as different values of friction characteristics would have to be adopted for individual belt elements.

7. References

[1] BOWDEN F. P.; TABOR D.: *The friction and lubrication of solids – Part II*. Oxford University Press, 1964.

[2] ČEPON G.; BOLTEŽAR M.: *Dynamics of a belt-drive system using a linear complementarity problem for the belt-pulley contact description*. Journal of Sound and Vibration, 319, 2009, pp. 1019–1035.

[3] ČEPON G.; MANIN L.; BOLTEŽAR M.: *Experimental identification of the contact parameters between a V-ribbed belt and a pulley*. Mechanism and Machine Theory, 45, 2010, pp. 1424–1433.

[4] ČEPON, G.; MANIN L.; BOLTEŽAR M.: *Introduction of damping into the flexible multibody belt-drive model: A numerical and experimental investigation*. Journal of Sound and Vibration, 324, 2009, pp. 283–296.

[5] Dahl P. R.: *A Solid Friction Model*. Report No. TOR-0158(3107-18)-1, Aerospace Corporation Report, 1968.

[6] DUDZIAK M.: *Przekładnie cięgnowe* (*Flexible-connector transmissions*). Wydawnictwo Naukowe PWN, Warszawa, 1997.

[7] EULER M. L.: *Remarques sur l'effect du frottement dans l'equilibre*. Mém. Acad. Sci., Berlin, 1762, pp. 265–278.

[8] FAWCETT J. N.: *Chain and belt drives – a review*. Shock Vibrations Digest, 13(5), 1981, pp. 5–12.

[9] JULIO G.; PLANTE J. S.: *An experimentally-validated model of rubber-belt CVT mechanics*. Mechanism and Machine Theory, 46, 2011, pp. 1037–1053.

[10] KIM D.; LEAMY M. J.; FERRI A. A.: *Dynamic Modeling and Stability Analysis of Flat Belt Drives Using an Elastic/Perfectly Plastic Friction Law*. ASME Journal of Dynamic Systems, Measurement, and Control, 133, 2011, pp. 1–10.

[11] KRAGEL'SKIJ I. V.; GITIS N. V.: *Frikcionnye avtokolebanija*. Akademija Nauk SSSR, Nauka, Moskva, 1987.

[12] LEAMY M. J.; WASFY T. M.: *Analysis of belt-drive mechanics using a creep-rate-dependent friction law*. Journal of Applied Mechanics, Trans. of ASME, 69, 2002, pp. 763–771.

[13] LEAMY M. J.; WASFY T. M.: *Dynamic finite element modeling of belt drives*. 18th Biennial Conference on Mechanical Vibration and Noise, ASME International 2001 DETC.

[14] LEAMY M. J.; WASFY T. M.: *Transient and Steady-State Dynamic Finite Element Modeling of Belt-Drives*. ASME Journal of Dynamic Systems, Measurement, and Control, 124, 2002, pp. 575–581.

[15] REYNOLDS O.: *Creep theory of belt drive mechanics*. The Engineer, 38, 1847.

[16] SCHINDLER T.; FRIEDRICH M.; ULBRICH H.: *Computing time reduction possibilities in multibody dynamics*. Multibody Dynamics: Computational Methods and Applications, Dordrecht, Springer, 23, 2011, pp. 239–259.

[17] THRELFALL D. C.: *The Inclusion of Coulomb Friction in Mechanisms Programs with Particular Reference to DRAM*. Mechanisms and Machine Theory, 13, 1978, pp.475–483.

[18] VOIGT W.: *Über innere Reibung fester Körper, insbesondere der Metalle*. Annalen der Physik, 283, pp. 671–693, 1892.

[19] MSC.ADAMS documentation.